

The imprints of reionization on the young Universe

Simona Gallerani
(ELTE, Budapest, Hungary)



in collaboration with: A. Ferrara, T. Roy Choudhury, P. Dayal, X. Fan, R. Salvaterra

In the last few years a possible tension has been identified between CMB and SDSS data, the former being consistent with an epoch of reionization $z_{\text{rei}} \sim 11$, the latter suggesting $z_{\text{rei}} \sim 6$. Long GRBs may constitute a complementary way to study the reionization process possibly probing $z > 6$. Moreover, an increasing number of LAEs are routinely found at $z > 6$. Here, two physically motivated and detailed reionization scenarios are presented: an Early Reionization Model (ERM) in which the intergalactic medium (IGM) is reionized at $z_{\text{rei}} \sim 7$, and a Late Reionization Model (LRM) in which overlapping occurs at $z_{\text{rei}} \sim 6$. We compare the results of our models with QSOs, GRBs and LAEs data.

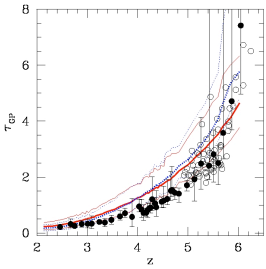


Fig 1: Evolution of the τ_{GP} for the ERM (solid red line) and LRM (blue dotted). Thick lines represent average results on 100 LOS, while the thin lines denote the upper and lower transmission extremes. Filled and empty circles are observational data from [13] and [3], respectively.

Modelling the Ly α forest

The ultraviolet (UV) radiation emitted by a QSO/GRB can suffer resonant Ly α scattering as it propagates through the intergalactic neutral hydrogen (HI). In this process, photons are removed from the line of sight (LOS) resulting in an attenuation of the source flux, the so-called Gunn-Peterson (GP) effect. We simulate the Ly α forest in absorption spectra by using the method described in [1]. In this model, mildly non-linear density fluctuations giving rise to spectral absorption features in the IGM are described by a Log-Normal distribution. For a given IGM equation of state, the mean HI fraction (x_{HI}) can be computed from photoionization equilibrium as a function of the photoionization rate, due to the UV background. These quantities are determined by the [2] model, based on two free parameters: (i) the star formation efficiency f_* , and (ii) the escape fraction f_{esc} of ionizing photons from galaxies. Currently, the available data can be explained by two different reionization histories: (i) an Early Reionization Model (ERM), characterized by a highly ionized IGM at $z > 6$, and (ii) a Late Reionization Model (LRM), in which $z_{\text{rei}} \sim 6$. Both ERM and LRM provide an excellent fit to the redshift evolution of the GP optical depth τ_{GP} (Fig. 1) and of x_{HI} (Fig. 2), experimentally deduced from the GP test.

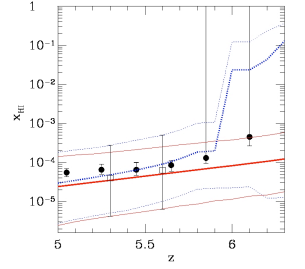


Fig 2: Evolution of x_{HI} for the ERM (solid red line) and LRM (blue dotted). Thick lines represent average results on 100 LOS, while the thin lines denote the upper and lower x_{HI} extremes. Filled circles represent estimates by [3], empty squares denote the results obtained in [4].

QSOs absorption spectra at $z \sim 6$

We test the predictions of our models by comparing statistically the properties of our simulated spectra with observations. Specifically, we concentrate on those regions of the spectra in which there is not transmitted flux (gaps). Gaps are defined as contiguous regions of the spectrum characterized by a transmitted flux $F_{\text{th}} < 0.1$ over rest-frame wavelength intervals $> 1 \text{ \AA}$. We introduce the Largest Gap Width Distribution (LGWD), a statistical analysis which quantifies the fraction of LOS characterized by the largest gap (LG) of a given width. These statistics have been applied to our simulated spectra and the results compared with observations (Fig. 3). We use observational data including 17 QSOs [3]. We divide the observed spectra into two redshift-selected sub-samples: the ‘‘Low-Redshift’’ (LR) sample ($5.7 < z_{\text{cm}} < 6$), and the ‘‘High Redshift’’ (HR) one ($6 < z_{\text{cm}} < 6.4$). From the LR sample we find $\log_{10} x_{\text{HI}} = -4.4 \pm 0.90$ at $z_{\text{mean}} = 5.3$, while by using the HR sample we constrain x_{HI} to be within $\log_{10} x_{\text{HI}} = -4.2 \pm 0.90$ at $z_{\text{mean}} = 5.6$. Although the predicted LGWD are quite similar for the two models considered, the ERM is in better agreement with observations. Moreover, in the HR a x_{HI} at $z \sim 6$ higher than that one predicted by the LRM would produce a lower (higher) fraction of LOS characterized by the LG smaller (higher) than 40 \AA with respect to observations. Thus, at $z \sim 6.3$, this study suggests $x_{\text{HI}} < 0.36$. See [4] for further details.

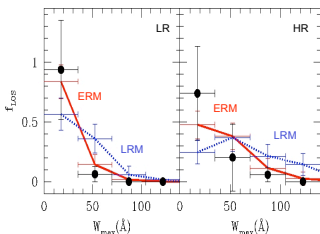


Fig 3: Largest Gap Width Distribution for the Low Redshift and High Redshift cases (left and right, respectively). Filled circles are obtained from [3] data; solid red (blue dotted) lines show ERM (LRM) results. Vertical error bars give the poissonian noise, horizontal error bars define the bin for the gap widths.

The case of GRB050904

We compare the predictions of our models with the optical afterglow spectrum of the GRB 050904, detected at $z = 6.3$ [5]. In this case, we derive the evolution of the LGWD, varying the flux threshold used to define gaps. We compute the probability that in the observed afterglow spectrum the LG, defined by F_{th} , is found within a given width range $[W_{\text{max}}, W_{\text{max}} + dW]$. We vary F_{th} between 0 and the maximum value of the detected flux. In Fig. 4, we compare our results with the GRB050904 spectrum. Note that we refer to the observed flux $F_{\text{obs}} = F(\nu)e^{-\tau}$, where $F(\nu) = \nu^\alpha t^\beta$, with $(\alpha, \beta) = (-1.25, -2.4)$ [6]. The point with arrow means that the gap size should be considered as an upper limit, since the corresponding dark region could be affected by the presence of a DLA [5]. It results that the ERM is more than 2 times more probable than the LRM in explaining observations, and that the observed LGW in the GRB 050904 afterglow spectrum are consistent with $x_{\text{HI}} = 6.4 \pm 0.3 \times 10^{-5}$. See [7] for further details.

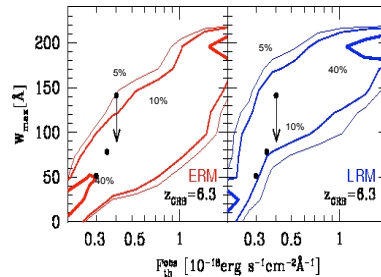


Fig 4: Isocontours of the probability (5%, 10%, 40%) that the afterglow spectrum associated with a GRB at $z = 6.3$, contains a largest gap of size in the range $[W_{\text{max}}, W_{\text{max}} + dW]$, for a flux threshold F_{th} . The left (right) panel shows the results for the ERM (LRM). The black points indicate the position in the $(W_{\text{max}}, F_{\text{th}}$) plane of GRB050904.

The LF of LAEs at $4.5 < z < 6.6$

A semi-analytical model of LAEs has been developed to compute the observed Ly α Luminosity $L_{\alpha} = e^{-\tau} L_{\alpha}^{\text{int}}$, where τ is computed starting from the x_{HI} predictions of the ERM/LRM and L_{α}^{int} is the intrinsic Ly α luminosity, obtained as follows: 1) by using the Sheth-Tormen mass function, we calculate the Star Formation Rate (SFR); 2) by using the population synthesis code *Starburst99*, we compute the number of ionizing photons for each SFR, and the relative L_{α}^{int} . Our model is based on two free parameters: (i) the fraction of baryonic matter that forms stars in a fraction of the Hubble time; (ii) $(1 - f_{\text{esc}})f_*$, where f_{esc} is the fraction of HI ionizing photons that escape the galaxy without causing any ionizations, and f_* the fraction of Ly α photons that escape the galaxy without being destroyed by dust. We compute the Ly α Luminosity Function (LF) at $z = 4.5, 5.7, 6.6$ and we calibrate our free parameters by matching the observed LF [8,9,10]. For both the ERM and LRM the LF data at $z = 4.5$, imply an extra Ly α line damping factor of ~ 0.25 , possibly due to dust; the ERM fits the observed LAE LF at $z = 5.7$ and 6.6 (Fig. 5) requiring no redshift evolution or mass dependence of the star formation efficiency; the LRM, instead, requires a physically uncomfortable drop of ~ 4.5 times in the SFR of the emitters from $z = 6.6$ to 5.7 . Thus, also in this case, the data favor a highly ionized Universe at $z \sim 6.6$ [11].

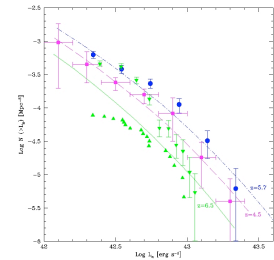


Fig 5: Cumulative LAEs luminosity function for the ERM. Points represent the data at three different redshifts: $z = 4.5$ [8] (squares), $z = 5.7$ [9] (circles), $z = 6.6$ [10] with downward (upward) triangles showing the upper (lower) limits. Lines refer to the model predictions at the same redshifts: $z = 4.5$ (dashed), $z = 5.7$ (dot-dashed), $z = 6.6$ (solid).

Conclusions

A cosmic reionization scenario (ERM) which simultaneously accounts for QSOs, GRBs and LAEs observational data has been presented. By comparing synthetic absorption spectra with a sample of 17 QSOs at $5.7 < z_{\text{cm}} < 6.4$ and with the GRB050904 detected at $z_{\text{cm}} = 6.3$, it results that the data seem to favor a highly ionized ($x_{\text{HI}} \sim 10^{-4.0}$) IGM at $z \sim 6$. The model, calibrated to match QSOs and GRBs data, is also successful in explaining the LF of LAEs at $4.5 < z_{\text{cm}} < 6.6$. The overall result points towards an extended reionization process which starts at $z \sim 11$ and completes at $z \sim 7$, in agreement with the recent WMAP5 data [12].